Water Transport Through Carbon Nanotubes with Defects

W.D. Nicholls*, M.K. Borg*, D.A. Lockerby** and J.M. Reese*

* Department of Mechanical & Aerospace Engineering,
University of Strathclyde, Glasgow G1 1XJ, UK
** School of Engineering, University of Warwick, Coventry CV4 7AL, UK
william.nicholls@strath.ac.uk

ABSTRACT

Non-equilibrium molecular dynamics simulations are performed to investigate how changing the number of structural defects in the wall of a (7,7) single-wall carbon nanotube (CNT) affects water transport and internal fluid dynamics. Structural defects are modelled as vacancy sites (missing carbon atoms). We find that, while fluid flow rates exceed continuum expectations, increasing numbers of defects lead to significant reductions in fluid velocity and mass flow rate. The inclusion of such defects causes a reduction in the water density inside the nanotubes and disrupts the nearly-frictionless water transport commonly attributed to CNTs.

Keywords: carbon nanotubes, molecular dynamics, water flow, defects

1 INTRODUCTION

Water transport through carbon nanotubes (CNTs) is currently subject to intense research through both experiments and molecular dynamics (MD) simulations. Both have shown that CNTs transport water at flow rates which are considerably higher than continuum expectations [1–3]. CNTs aligned in a membrane have major potential for selective material separation, with one of the most promising applications being sea water desalination [3]. However very few MD studies include defects when modelling CNTs: pristine, defect-free CNTs are commonly studied. This leaves a gap in our understanding of water transport through these nanoscale structures.

CNT defects are, however, commonplace in experiments as it is very difficult to manufacture pristine CNTs, e.g. during the uncapping procedure (typically plasma oxidation) functionalisation defects are produced that have been shown through simulation [4, 5] and experiment [6] to reduce water transport rates. Other defect types that can occur during the manufacturing process are: Stone-Wales topological defects, adatoms, and vacancy sites. Vacancy sites are structural defects that can be mono-vacancies or multi-vacancies in the walls of CNTs [7, 8]. The properties of CNTs, including fluid transport, will be affected by the presence of these defects on their inner-walls and tips.

We have shown in a previous study [9] that the flow enhancement factor, defined as the ratio of the MD simulated mass flow rate to the hydrodynamic prediction, increases linearly with CNT length for a fixed pressure difference. If this trend continues up to the lengths used in experiments, which can be 2-5 μm, then the flow enhancement factor would far exceed those reported from experiments. The inclusion of defects in the present MD study may help to understand the role of defects in flow enhancement.

There are many published papers that assess the change in mechanical properties of CNTs due to the inclusion of defects. Yang *et al.* [8] included functionalised, Stone-Wales, and vacancy type defects in their MD study of the tensile strength of CNTs, and found that the inclusion of such defects produced weaker CNTs. They also found that the tensile strength of the CNT became comparable to the lower values reported in experiments, rather than the exceptionally high theoretical values found from calculations assuming defect-free CNTs.

There are only a few reports of the effect of CNT defects on fluid transport. Li *et al.* [10] modelled using MD the permeation of water through CNTs with Stone-Wales defects. They found that the flow rate decreased with an increasing number of such defects. Kotsalis *et al.* [11] performed MD simulations of water inside CNTs doped with oxygen and hydrogen, and found that the wetting contact angle of water reduced with increasing doping sites, making the CNTs more hydrophilic. CNT functionalisation (tip and core) reduces water transport rates, as discussed previously. To the authors' knowledge, there has been no report of the effect of CNT vacancy site defects on the water transport rate.

In this paper, we use MD simulations to investigate water transport through (7,7) single-wall CNTs, which have a diameter of 0.96 nm, with a fixed length of 25 nm. We examine how changing the number of vacancy defects affects the fluid flow behaviour. The number of defects is quantified by the percentage of carbon atoms which are removed from the original, defect-free structure. Only (7,7) CNTs are considered in this study since it has been shown previously that this is a good choice for desalination applications: they possess the required diameter to reject 95% of salt ions and still allow a high

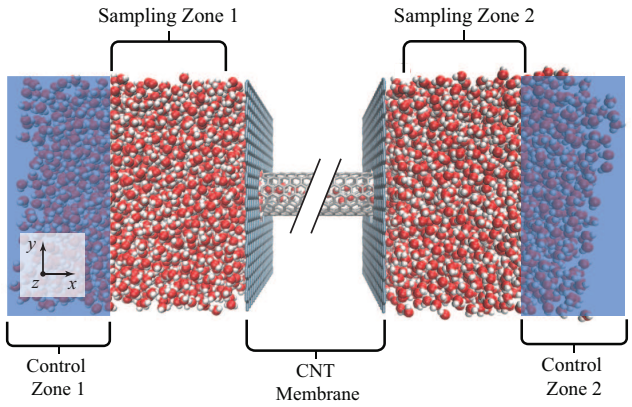

Figure 1: Simulation domain.

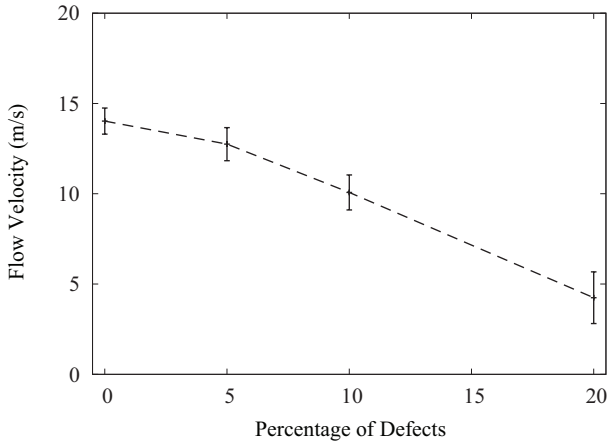

Figure 2: Variation of flow velocity with percentage of CNT defects for a 200 MPa pressure difference.

flow rate of water to pass through [3].

A single-wall CNT with missing carbon atoms would not be a stable structure on its own due to the presence of unsaturated bonds, however such a case is plausible for a multi-wall CNT with an inner shell having the diameter of a single-wall CNT with vacancy sites. For desalination applications, semipermeable CNT membranes will most likely be composed of multi-wall CNTs [12]. Four cases are considered herein: 0%, 5%, 10%, and 20% vacancy defect densities, and we report the effect these have on fluid flow rates, fluid densities and axial pressure profiles.

2 SIMULATION METHODOLOGY

Our MD simulations are performed using *mdFoam* [13–15], a parallelised non-equilibrium molecular dynamics solver that is open-source and available to download from [16]. The motion of molecules is governed by Newton's second law, and the equations of motion are integrated using the Verlet leapfrog scheme. A time-step of 1 fs is used in all the following simulations. The TIP4P water model is used and the carbon-water interaction is represented by the LJ potential of Werder *et al.* [17]. Electrostatic and Lennard-Jones interactions are smoothly truncated at 1.0 nm.

The configuration of our pressure-driven flow simulation domain is shown in Fig. 1 and is similar to our previous study [9]. Two graphene sheets are positioned at the inlet and outlet of the CNT to form a simplified CNT membrane representation. The CNT and graphene sheets are modelled as rigid structures. Periodic boundary conditions are employed in the y- and z-directions, while non-periodic boundary conditions are applied in the x-direction: the left-hand boundary is a specular-reflective wall, while the right-hand boundary deletes molecules upon collision. The deletion patch creates an open system [18] and prevents the simulation from being over-constrained. A pressure difference of 200 MPa is applied across the membrane in all our simulations. Berendsen thermostats are applied to both fluid reservoirs to maintain a constant temperature of 298 K; the fluid is not controlled inside the CNT.

The upstream pressure is controlled using a proportional-integral-derivative (PID) control feedback loop algorithm, in addition to adaptive control of mass-flux at the inlet; both are discussed in detail in [9]. The downstream pressure is controlled using a pressure-flux technique [19], which applies an external force to all molecules in control zone 2 that corresponds to the target pressure. By controlling pressure in this way, it creates an open boundary allowing a fluid flux to pass through the system and the required reservoir pressures can be specified explicitly. The same reservoir conditions are adopted in each simulation run. The maximum variation in the applied pressure difference was measured to be 1.76 MPa. All data presented in this paper is from a 4 ns averaging period.

Single carbon atoms are removed at random places within the original defect-free nanotube structure, until the required percentage of defects is reached. Higher-order vacancy clusters (groups of three or four single defects) occur in the 10% and 20% defect cases. The modelling of the CNT as a rigid structure may therefore introduce errors in cases with high defect densities, and this will be the scope of future work.

3 RESULTS AND DISCUSSION

The average fluid streaming velocities for different percentages of vacancy defects under the same applied pressure difference are shown in Fig. 2. We find that increasing the number of defects reduces the average fluid velocity through the nanotube. Small numbers of defects (5%) cause the fluid velocity to reduce by ∼10%, however greater quantities of defects caused a reduction of ∼70%. Defect densities are likely to be less than 10% in CNTs [8] and these results show a significant reduction in fluid velocity may be present in this range. The fluid velocity inside the defect-free CNT is in agreement

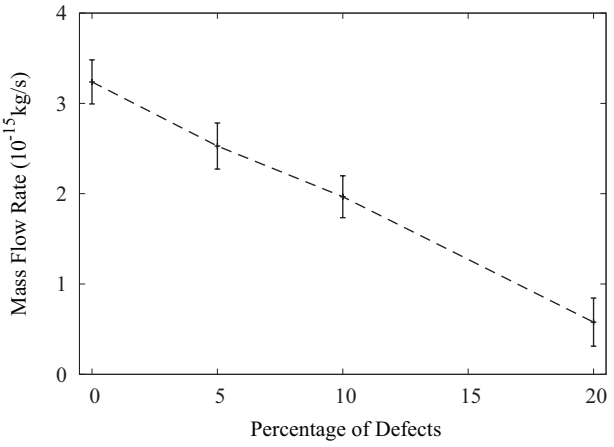

Figure 3: Relationship between flow rate and percentage of CNT defects for a 200 MPa pressure difference.

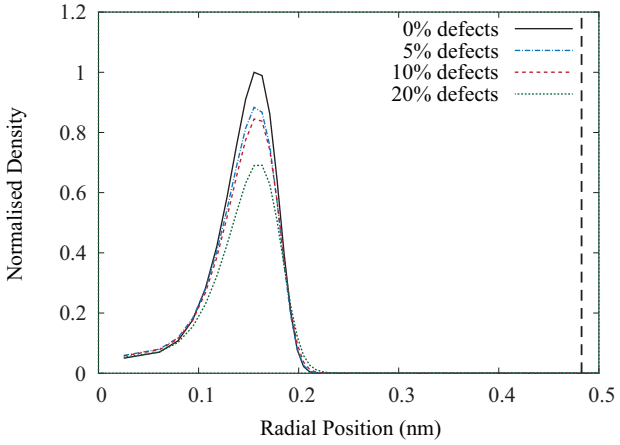

Figure 4: Normalised radial water density distributions for CNTs with different numbers of defects present. The vertical dashed line indicates the position of the CNT surface.

with previous results [9, 20].

The net mass flow rate is measured by averaging the number of molecules which cross five equidistant planes inside each CNT over a prescribed time period, and is shown in Fig. 3. The mass flow rate decreases with increasing numbers of defects, however the effect of including vacancy defects at lower densities is more influential: ∼20% reduction in flow rate for 5% defects, and ∼80% reduction for 20% defects. Increasing the number of vacancy defects causes a roughly linear reduction in the resultant mass flow rate, whereas the flow velocity demonstrated a non-linear relationship. One would expect a similar trend to exist for both fluid velocity and mass flow rate since the CNTs have the same diameter – which means that the internal fluid density may be changing, which is now discussed.

The mean distribution of radial water density for each CNT is shown in Fig. 4. The average density profile for each case is annular and the peak density occurs at the same radial position, which indicates that the

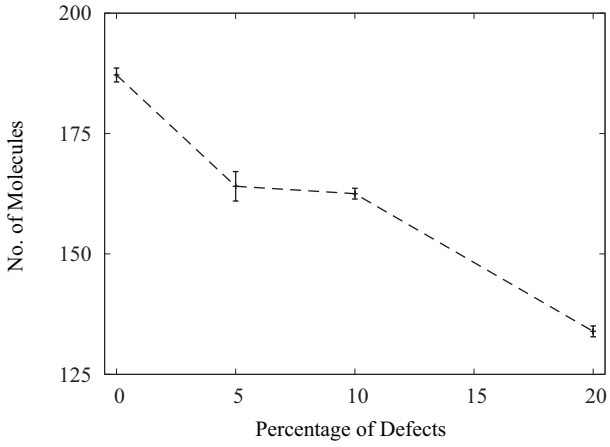

Figure 5: Relationship between the average number of water molecules in the CNT and percentage of defects.

inclusion of vacancy defects has not altered the CNT effective radius. The radial density decreases with increasing numbers of defects, which means that the water molecules are not as tightly packed in CNTs with vacancy defects. The total fluid density is dependent upon the definition of the occupied volume of the CNT, for which there is no consistency in the literature [21], but we know that this volume is the same for each CNT in this study since the effective radius and length are consistent in each case. Therefore the total fluid density can be described by the total number of water molecules contained within each CNT, and is shown in Fig. 5. The average number of water molecules inside each CNT decreases with increasing defects; the inclusion of vacancy site defects disrupts the optimum internal fluid structuring so that the number of water molecules that can occupy the CNT is reduced. The large reduction in density in the 5% defect case is responsible for the differences between the relationships for flow velocity and mass flow rate.

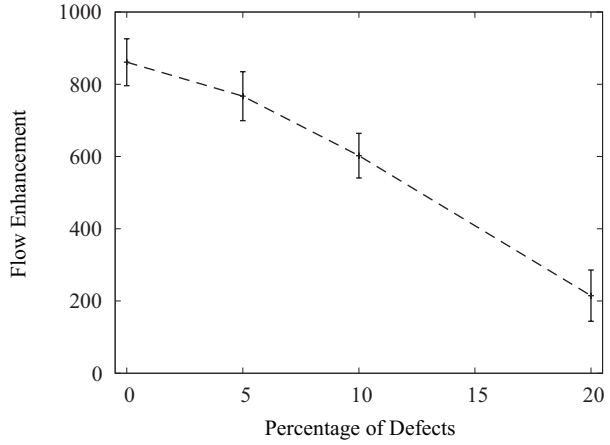

Figure 6: Flow enhancement values for different percentages of defects, for a 25 nm CNT under a 200 MPa pressure difference.

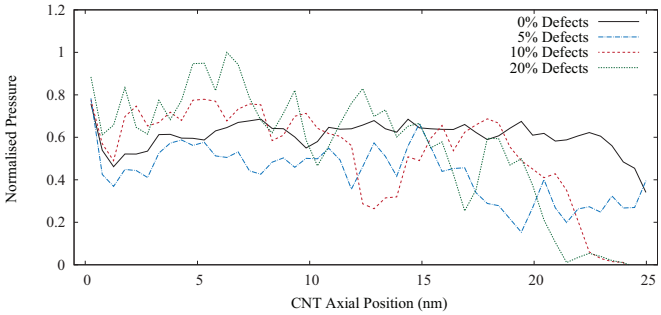

Figure 7: Axial pressure profile of water in CNTs with defects.

The measured flow rates can be compared to predicted hydrodynamic flow rates via the no-slip Poiseuille relation for flow in a cylindrical pipe:

$$\dot{m} = \frac{\pi r^4 \rho \Delta P}{8 \mu L}, \tag{1}$$

where r is the radius of the CNT, ΔP is the pressure difference, ρ is the water density, μ is the dynamic viscosity, and L is the CNT length. We take the radius within which 95% of the fluid resides, which was found to be 0.186 nm. Bulk properties for ρ and μ for water at 298 K are used in the defect-free case and ρ is calculated to include the reductions in density experienced in CNTs with defects. The flow enhancement factor for each case is shown in Fig. 6. This non-linear reduction in the flow enhancement factor with increasing number of site defects is caused by a combined lower fluid density and flow velocity.

To understand why the average fluid velocity decreases when defects are present, we must consider the axial fluid pressure profile along each CNT, shown in Fig. 7. The presence of vacancy site defects causes the pressure profiles to deviate from the frictionless profile present in the 0% defect case (also reported in [9]). The flow becomes more like flow in a rough pipe, indicated by the greater pressure losses experienced in cases with defects and this reduces the average fluid velocity.

4 CONCLUSIONS

Non-equilibrium MD simulations have shown how changing the number of vacancy site defects within the surface of a (7,7) CNT affects the internal flow dynamics. Including defects reduces the fluid velocity and mass flow rate rate considerably. Mass flow rate is further affected by a reduction in the overall fluid density caused by the presence of the defects. The inclusion of vacancy sites disrupts the smooth, continuous potential energy landscape a CNT provides, causing greater pressure losses along it, which reduces the overall fluid velocity. Flow enhancement factors are reduced significantly with increasing numbers of defects, which may account to some extent for the over-prediction of fluid flow rates in MD simulations using pristine CNTs when compared with experimental results.

5 ACKNOWLEDGEMENTS

The authors thank Davide Mattia of the University of Bath for useful discussions. This work is funded in the UK by the Engineering and Physical Sciences Research Council under grant EP/F002467/1, and by the Institution of Mechanical Engineers. JMR would like to thank the Royal Academy of Engineering and the Leverhulme Trust for support through a Senior Research Fellowship.

REFERENCES

[1] M. Majumder, N. Chopra, R. Andrew, and B. J. Hinds. Nanoscale hydrodynamics: enhanced flow in carbon nanotubes. *Nature*, 438:44, 2005.

[2] J. K. Holt, H. G. Park, Y. Wang, M. Stadermann, A. B. Artyukhin, C. P. Grigoropoulos, A. Noy, and O. Bakajin. Fast mass transport through sub-2-nanometer carbon nanotubes. *Science*, 312(5776):1034–1037, 2006.

[3] B. Corry. Designing carbon nanotube membranes for efficient water desalination. *Journal of Physical Chemistry B*, 112(5):1427–1434, 2008.

[4] B. Corry. Water and ion transport through functionalised carbon nanotubes: implications for desalination technology. *Energy & Environmental Science*, 4:751–759, 2011.

[5] M. Majumder and B. Corry. Anomalous decline of water transport in covalently modified carbon nanotube membranes. *Chemical Communications*, 47:7683–7685, 2011.

[6] M. Majumder, N. Chopra, and B. J. Hinds. Mass transport through carbon nanotube membranes in three different regimes: Ionic diffusion and gas and liquid flow. *ACS Nano*, 5(5):3867–3877, 2011.

[7] A. Hashimoto, K. Suenaga, A. Gloter, K. Urita, and S. Iijima. Direct evidence for atomic defects in graphene layers. *Nature*, 430(7002):870–873, 2004.

[8] M. Yang, V. Koutsos, and M. Zaiser. Size effect in the tensile fracture of single-walled carbon nanotubes with defects. *Nanotechnology*, 18(15):155708, 2007.

[9] W. D. Nicholls, M. K. Borg, D. A. Lockerby, and J. M. Reese. Water transport through (7,7) carbon nanotubes of different lengths using molecular dynamics. *Microfluidics and Nanofluidics*, 2011. to be published.

[10] S. Li, P. Xiu, H. Lu, X. Gong, K. Wu, R. Wan, and H. Fang. Water permeation across nanochannels with defects. *Nanotechnology*, 19(10):105711, 2008.

[11] E. M. Kotsalis, E. Demosthenous, J. H. Walther, S. C. Kassinos, and P. Koumoutsakos. Wetting of

doped carbon nanotubes by water droplets. *Chemical Physics Letters*, 412(4-6):250–254, 2005.

[12] D. Mattia and Y. Gogotsi. Static and dynamic behavior of liquids inside carbon nanotubes. *Microfluidics and Nanofluidics*, 5:289–305, 2008.

[13] G. B. Macpherson, M. K. Borg, and J. M. Reese. Generation of initial molecular dynamics configurations in arbitrary geometries and in parallel. *Molecular Simulation*, 33(15):1199 – 1212, 2008.

[14] G. B. Macpherson and J. M. Reese. Molecular dynamics in arbitrary geometries: Parallel evaluation of pair forces. *Molecular Simulation*, 34(1):97 – 115, 2008.

[15] M. K. Borg, G. B. Macpherson, and J. M. Reese. Controllers for imposing continuum-to-molecular boundary conditions in arbitrary fluid flow geometries. *Molecular Simulation*, 36(10):745 – 757, 2010.

[16] OpenFOAM Foundation. http://www.openfoam.org, 2011.

[17] T. Werder, J. H. Walther, R. Jaffe, T. Halicioglu, and P. Koumoutsakos. On the water-carbon interaction for use in molecular dynamics simulations of graphite and carbon nanotubes. *Journal of Physical Chemistry B*, 107(41):1345–1352, 2003.

[18] E. G. Flekkøy, R. Delgado-Buscalioni, and P. V. Coveney. Flux boundary conditions in particle simulations. *Physical Review E*, 72(2):026703, 2005.

[19] G. D. Fabritiis, R. Delgado-Buscalioni, and P. V. Coveney. Multiscale modeling of liquids with molecular specificity. *Physical Review Letters*, 97(13):134501, 2006.

[20] J. A. Thomas and A. J. H. McGaughey. Water flow in carbon nanotubes: transition to subcontinuum transport. *Physical Review Letters*, 102(18):184502, 2009.

[21] A. Alexiadis and S. Kassinos. Molecular simulation of water in carbon nanotubes. *Chemical Reviews*, 108(12):5014–5034, 2008.